

Analyst

Accepted Manuscript



This is an *Accepted Manuscript*, which has been through the Royal Society of Chemistry peer review process and has been accepted for publication.

Accepted Manuscripts are published online shortly after acceptance, before technical editing, formatting and proof reading. Using this free service, authors can make their results available to the community, in citable form, before we publish the edited article. We will replace this *Accepted Manuscript* with the edited and formatted *Advance Article* as soon as it is available.

You can find more information about *Accepted Manuscripts* in the [Information for Authors](#).

Please note that technical editing may introduce minor changes to the text and/or graphics, which may alter content. The journal's standard [Terms & Conditions](#) and the [Ethical guidelines](#) still apply. In no event shall the Royal Society of Chemistry be held responsible for any errors or omissions in this *Accepted Manuscript* or any consequences arising from the use of any information it contains.

1
2
3
4 **In vivo fluorescent sensing of salicylate-induced change of zinc ion in**
5 **auditory cortex of rat brain**
6
7

8
9 Qin Jiang,[†] Zijian Guo,[‡] Yao Zhao,[†] Fuyi Wang,[†] Lanqun Mao^{†,*}
10

11
12 [†]*Beijing National Laboratory for Molecular Sciences, Key Laboratory of Analytical*
13 *Chemistry for Living Biosystems, Institute of Chemistry, the Chinese Academy of Sciences,*
14 *Beijing 100190, P. R. China.*
15

16
17 [‡]*State Key Laboratory of Coordination Chemistry, Coordination Chemistry Institute, School*
18 *of Chemistry and Chemical Engineering, Nanjing University, Nanjing 210093, P. R. China.*
19
20
21
22
23
24
25
26
27
28
29
30
31
32
33
34
35
36
37
38
39
40
41
42
43
44
45
46
47
48
49
50
51
52

53 *Corresponding Author. Fax: (+86)-10-6255-9373; Email: lqmao@iccas.ac.cn
54
55
56
57
58
59
60

1
2
3
4 **Abstract:** This study demonstrates a fluorescent method for in vivo sensing of the dynamic
5
6 change of Zn^{2+} concentration in auditory cortex microdialysate induced by salicylate with
7
8 N^{\prime} -(7-nitro-2,1,3-benzoxadiazole-4-yl)- N,N,N^{\prime} -tris(pyridine-2-ylmethyl) ethane-1,2-diamine
9
10 (NBD-TPEA) as a probe. The excellent property of NBD-TPEA probe makes it possible to
11
12 achieve a high selectivity for Zn^{2+} sensing with the co-existence of amino acids and other
13
14 metal ions as well as the species commonly existing in the cerebral system. To validate the
15
16 method for in vivo fluorescence sensing of Zn^{2+} in rat brain, we pre-mix the microdialysates
17
18 in vivo sampled from auditory cortex with NBD-TPEA probe and then perfuse the mixtures
19
20 into a fluorescent cuvette for continuous-flow fluorescence detection. The method
21
22 demonstrated here shows a linear relationship between the signal output and Zn^{2+}
23
24 concentration within the concentration range from 0.5 μ M to 4 μ M, with a detection limit of
25
26 156 nM ($S/N = 3$). The basal level of extracellular Zn^{2+} in auditory cortex microdialysate is
27
28 determined to be $0.52 \pm 0.082 \mu$ M ($n = 4$). This value is increased by the injection of 100
29
30 mg/mL of salicylate (1 μ L/min, 5 min, i.p.), reaches a peak at the time point of 90 min, and
31
32 levels off with time. Such an increase is attenuated by the injection of MK-801, a potent and
33
34 specific NMDA receptor antagonist, after the pre-injection of 100 mg/mL salicylate for 5
35
36 min. This study offers a fluorescent method for in vivo sensing of Zn^{2+} in rat brain that could
37
38
39
40
41
42
43
44
45
46
47
48
49
50
51
52
53
54
55
56
57
58
59
60

1
2
3
4 Understanding of the chemical processes involved in the salicylate-induced
5 physiological and pathological events is of great importance since, as one kind of
6 anti-inflammatory component of aspirin, salicylate has been widely used to treat various
7 ailments.¹ However, excessive salicylate would induce a series of diseases, such as allergic
8 reactions, hepatic and renal dysfunction, tinnitus and hearing loss.² For example, early
9 attempts have demonstrated that systemic injection of 250 mg/kg of salicylate can
10 significantly reduce the sound evoked field output of the rat cochlea, in which salicylate
11 competes with the contribution of cytoplasmic chloride to nonlinear capacitance of sensory
12 outer hair cells.³ On the other hand, in the salicylate-induced physiological and pathological
13 events, a comprehensive chemical process has been proposed to be involved.⁴ For instance,
14 the injection of high doses of salicylate evokes excessive glutamate efflux from inner hair
15 cells into cochlear, which not only results in cochlea excitotoxicity but also leads to
16 temporary hearing threshold shift.⁵ Moreover, the injection of salicylate could decrease
17 cochlear perilymph ascorbate of guinea pigs, as demonstrated in our early study,⁶ suggesting
18 that ascorbate may be involved in the chemical processes of the salicylate-induced tinnitus.
19 In spite of these early studies, the chemical processes involved in the salicylate-induced
20 physiological and pathological events remain to be further explored and understood.

21
22
23
24
25
26
27
28
29
30
31
32
33
34
35
36
37
38
39
40
41
42 As one kind of the most abundant transition metal elements that presents in all organs
43 and bodies, Zn^{2+} has been demonstrated to play critical roles in many physical and
44 pathological processes, especially in brain function activity.⁷ For instance, in central nervous
45 system, Zn^{2+} acts as an important endogenous neuromodulator for glutamate transmission.⁸
46 During forebrain ischemia, considerable Zn^{2+} was reported to release from synaptic vesicles
47 of glutamatergic neuronal terminal to extracellular fluid, which would cause neuronal death.⁹
48 In spite of these attempts, a close survey of literature indicates that there is no report on the
49 role of Zn^{2+} that plays in the salicylate-induced physiological and pathological events. In this
50
51
52
53
54
55
56
57
58
59
60

1
2
3 context, a method that is capable of in vivo sensing of Zn^{2+} level remains very essential.
4
5
6 However, the high chemical complexity inherent in the cerebral system, the requirement of
7
8 spatial resolution of the investigation on chemical issues in the physiological and
9
10 pathological events, as well as the less theoretical and instrumental demanding of
11
12 neurotechnologies unfortunately render difficulties in applying the methods reported so far
13
14 for Zn^{2+} measurement.¹⁰
15
16

17
18 Very recently, one of our authors has demonstrated that the NBD-TPEA probe displays
19
20 a high selectivity and sensitivity towards Zn^{2+} due to its strong affinity of all nitrogen atoms
21
22 of pyridine and amine towards Zn^{2+} .¹¹ Such a property of NBD-TPEA probe potentially
23
24 enables its promising application for effective sensing of Zn^{2+} in the cerebral system. To
25
26 explore such potentiality, we sample the brain dialysates with in vivo microdialysis
27
28 technique and pre-mix the microdialysates with the fluorescent probe and finally perfuse the
29
30 mixtures into a cuvette for continuous-flow fluorescence detection, as shown in Scheme 1.
31
32 The combination of sample pre-mixing with continuous-flow fluorescence detection
33
34 facilitates signal readout recording in a continuous-flow system, eliminates background
35
36 contamination, and minimizes fluorescent bleaching, while to some extent warrants the time
37
38 resolution. The method demonstrated here is highly selective and sensitive and could thus be
39
40 used for monitoring the dynamic change in Zn^{2+} concentration involved in various brain
41
42 function activity such as salicylate-induced physiological and pathological events.
43
44
45
46
47

48 **Experimental**

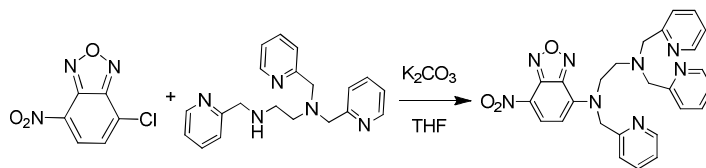
49 **Chemicals and solutions**

50
51 Dopamine (DA), lactate, glucose, sodium ascorbate (AA), uric acid (UA),
52
53 3,4-dihydroxyphenylacetic acid (DOPAC), 5-hydroxytryptamine (5-HT), dizocipine
54
55 [(+)-5-methyl-10, 11-dihydro-5H-dibenzo [a, d] cyclohepten-5, 10-imine] maleate (MK-801),
56
57
58
59
60

and amino acids (99%) were all purchased from Sigma-Aldrich. Sodium salicylate was obtained from Sinopharm Chemical Reagent Co., Ltd. Other chemicals were of at least analytical grade and used as received. Artificial cerebrospinal fluid (aCSF) used as the perfusion solution for in vivo microdialysis and in vitro experiments was prepared by mixing NaCl (126 mM), KCl (2.4 mM), KH₂PO₄ (0.5 mM), MgCl₂ (0.85 mM), NaHCO₃ (27.5 mM), Na₂SO₄ (0.5 mM), and CaCl₂ (1.1 mM) in Milli-Q water and the solution pH was adjusted to 7.4. All aqueous solutions were prepared with Milli-Q water (18.2 MΩ·cm).

Synthesis of NBD-TPEA

Synthesis of NBD-TPEA probe was conducted with the a procedure reported previously.¹¹ Briefly, N,N,N'-Tris(pyridine-2-ylmethyl) ethane-1,2-diamine (TPEA, 2754 mg, 8.26 mmol), K₂CO₃ (1142 mg, 8.26 mmol), and 4-chloro-7-nitro-2,1,3-benzoxiadiazole (4-CINBD, 1814 mg, 9.18 mmol) were mixed in 200 mL of tetrahydrofuran (THF) and the mixture was stirred overnight at room temperature. After that, the solvent was collected and evaporated under vacuum. The crude product obtained was chromatographed on silica gel by eluting with acetate/methanol (v/v, 8:1) to give an orange oil product with 63% yield.



In vivo microdialysis and fluorescent detection

Surgeries for in vivo microdialysis were performed as reported previously.¹² Adult male Sprague-Dawley rats (350-400 g) were purchased from Center of Health Science, Peking University and housed on a 12:12 h light-dark scheduler with food and water *ad libitum*. The animals were anaesthetized with chloral hydrate (345 mg/kg, i.p.) and positioned onto a stereotaxic frame. The microdialysis guide cannulas were carefully implanted in the auditory cortex (AP = -4.0 mm, L = 6.5 mm from bregma, V = 2.0 mm from the surface of the skull)

1
2
3 using standard stereotaxic procedures.¹³ The guide cannula was in place with three skull
4 screws and dental acrylic. Stainless steel dummy blockers were inserted into the guide
5 cannulas and fixed until the insertion of the microdialysis probe (CMA, dialysis length, 2
6 mm; diameter, 0.24 mm). Throughout the surgery, the body temperature of the animals was
7 maintained at 37 °C with a heating pad. Immediately after the surgery, the rats were placed
8 into a warm incubator individually until they recovered from the anesthesia. The rats were
9 allowed to recover for at least 24 h before in vivo microdialysis sampling. Prior to in vivo
10 fluorescent measurements, the microdialysis probe was implanted in the auditory cortex and
11 was allowed to equilibrate for at least 90 min by continuously perfusing aCSF at 1 $\mu\text{L min}^{-1}$.
12
13
14
15
16
17
18
19
20
21
22
23

24 In vitro fluorescent spectrum was recorded on a Hitachi F-4600 spectrometer (Hitachi
25 Co. Ltd. Japan) with a Xe lamp as the excitation source at room temperature. In vivo
26 continuous-flow fluorescence detection was performed in a RF-20A xs fluorescence detector
27 cell (Shimadzu Co. Ltd., Japan) with Xe lamp as the excitation source at room temperature.
28 The excitation wavelength was set as 469 nm, and the emission wavelength was set as 550
29 nm. To detect Zn^{2+} in the microdialysates in vivo sampled from the auditory cortex, we first
30 mixed 30 μL of auditory cortex microdialysates with 30 μL of NBD-TPEA (10 μM)
31 dissolved in DMSO/aCSF (v/v, 1:99, pH 7.4). After 5 min, the mixtures were perfused into a
32 fluorescence cell with microinjection pump (CMA 100, CMA Microdialysis AB, Stockholm,
33 Sweden) at a perfusion of rate of 3 $\mu\text{L min}^{-1}$ for continuous-flow fluorescent detection. The
34 basal level of Zn^{2+} in the microdialysates was obtained from the fluorescence response of the
35 mixtures containing microdialysates and NBD-TPEA probe (normal group). To study the
36 change of Zn^{2+} level in the microdialysates induced by salicylate injection, 100 mg/mL of
37 sodium salicylate dissolved in phosphate buffer (0.1 M, pH 7.4) was injected into the rats
38 (350 mg/kg, i.p.). Such a dose was reported to produce an animal model of tinnitus.^{3a,b} The
39 microdialysates were collected, mixed and detected with the same procedures employed for
40
41
42
43
44
45
46
47
48
49
50
51
52
53
54
55
56
57
58
59
60

1
2
3 the microdialysates from the normal group (salicylate group). To elucidate the
4 salicylate-induced change of Zn^{2+} level, in the separate experiments, we injected 1 mg/mL
5 MK-801 dissolved in phosphate buffer (0.1 M, pH 7.4) into the animals (5 mg/kg, i.p.) after
6 the animals were injected with 100 mg/mL salicylate for 5 min, and the microdialysates were
7 thus collected, mixed, and detected with the same method employed for the normal and
8 salicylate groups (Sal/MK-801 group). During the surgery and in vivo microdialysis
9 sampling, the body temperature of the animals was maintained at 37 °C with a heating pad
10 and anesthetic was supplemented if necessary.

21 ICP-MS analysis

22 Inductively coupled plasma mass spectrometry (ICP-MS) was carried out on an Agilent
23 7700x series ICP-MS instrument. For ICP-MS analysis, 20 μ L of the microdialysate was
24 diluted to 2 mL with Milli-Q water. Agilent ICP-MS calibration standards (multi-element)
25 was used for preparing the calibration curves, of which Zn^{2+} concentrations were 0, 0.02, 0.1,
26 0.5, 1, 5, 10, 50 and 100 ppb (μ g/mL), and Cd^{2+} concentration were 0, 0.001, 0.01, 0.1, 1 and
27 10 ppb (μ g/mL). The isotope detected was ^{66}Zn and ^{111}Cd , and both readings were made in
28 He gas mode.

41 Results and discussion

44 Fluorescent response and selectivity

45 In DMSO/aCSF (v/v, 1:99, pH 7.4) mixture, NBD-TPEA itself shows a weak
46 fluorescence with λ_{ex} and λ_{em} at 469 nm and 550 nm, respectively, as shown in Fig. 1 A. The
47 weak emission could be attributed to the presence of two amine groups at TPEA (Fig. 1 B,
48 inset, red dash circle) as reported previously;¹¹ TPEA connects to the
49 4-amino-7-nitro-2,1,3-benzoxadiazole (ANBD) fluorophore via an ethylene group and thus
50
51
52
53
54
55
56
57
58
59
60

1
2
3
4 quenches the emission of ANBD fluorophore via a space photoinduced electron transfer
5 (PET) process. However, when Zn^{2+} was added into the mixture of DMSO/aCSF containing
6 NBD-TPEA, the fluorescent emission intensity of NBD-TPEA was largely enhanced, as
7
8 displayed in Fig. 1 B (red curve). Such an enhancement was mainly caused by the PET block
9
10 effect induced by the coordination of Zn^{2+} to all N atoms of TPEA, which leads to the
11
12 recovery of the fluorescence of ANBD fluorophore.¹¹ In addition to its application for Zn^{2+}
13
14 imaging in living cells with excellent biocompatibility and cell permeability,¹¹ this
15
16 mechanism is envisaged to be particularly useful for in vivo sensing of Zn^{2+} in the cerebral
17
18 system, as described below.
19
20
21
22

23
24 To explore such possibility, we systematically studied the selectivity of the method for
25
26 Zn^{2+} sensing over other kinds of metal ions, amino acids, and physiologically important
27
28 species in the cerebral system. To do this, each kind of the species was separately added into
29
30 10 μ M of NBD-TPEA in the DMSO/aCSF mixture. As displayed in Fig. 2, no obvious
31
32 fluorescence enhancement was observed upon the addition of each kind of metal ions, (with
33
34 an exception of the addition of Zn^{2+} and Cd^{2+}) (A), amino acids (B), and physiologically
35
36 important species (C). We also studied the effect of metal ions, amino acids and
37
38 physiologically important species on the Zn^{2+} -enhanced fluorescent intensity of NBD-TPEA
39
40 and found that negligible signal changes were observed when each kind of metal ions (Fig.
41
42 S1), amino acids (Fig. S2), and physiologically important species (Fig. S3) was added into
43
44 the mixture of 10 μ M of NBD-TPEA and 10 μ M of Zn^{2+} in DMSO/aCSF. However, the
45
46 addition of Cd^{2+} into the same mixture clearly decreases the fluorescent intensity (data not
47
48 shown), which may be caused by the competitive coordination of Cd^{2+} and Zn^{2+} with
49
50 NBD-TPEA. Note that, the interference of Cd^{2+} was not considered here because of its low
51
52 level in the brain microdialysate (i.e., at a nanomolar level), as determined with the
53
54 traditional ICP-MS in our study (data not shown). Furthermore, no significant change of the
55
56
57
58
59
60

1
2
3
4 fluorescence response of 10 μM NBD-TPEA in DMSO/aCSF (v/v, 1:99, pH 7.4) at 550 nm
5
6 was observed upon consecutive excitation with 469 nm laser light for 60 min with an
7
8 interval of 1 min (data not shown), suggesting the good photostability of NBD-TPEA probe
9
10 employed in this study. The high selectivity and excellent photostability of the NBD-TPEA
11
12 probe form a strong basis for in vivo sensing of Zn^{2+} in the cerebral system.
13
14

15 16 17 **Fluorescent sensing of Zn^{2+}**

18
19 In order to validate the selective fluorescent mechanism demonstrated above for in vivo
20
21 sensing of Zn^{2+} in rat brain, we premixed the brain microdialysates with the probe and
22
23 perfused the resulting mixtures into a fluorescent cuvette with a volume as small as 30 μL
24
25 for continuous-flow fluorescent sensing (Scheme 1). With the method, we obtained a time
26
27 resolution of 30 min (30 μL , with 1 $\mu\text{L}/\text{min}$ as a perfusion rate for in vivo microdialysis).
28
29 Such a time resolution, although remained to be further improved in our future study, could
30
31 meet the requirement for understanding the chemical process involved in the
32
33 salicylate-induced physiological and pathological events such as tinnitus since previous
34
35 attempts have demonstrated that the development of salicylate-induced tinnitus was a slow
36
37 process.^{4a,b} Moreover, the method demonstrated here also facilitates the fluorescent signal
38
39 readout recording with less fluorescence bleaching because of the easily switchable property
40
41 and continuous-flow feature of the samples in the micro-volume fluorescent cuvette. As
42
43 displayed in Fig. 3, the method shows a well-defined response toward Zn^{2+} and the relative
44
45 fluorescence intensity $((F-F_0)/F_0)$ was linear with the concentration of Zn^{2+} with a dynamic
46
47 linear range within the concentration range from 0.5 μM to 4 μM ($(F-F_0)/F_0 = 0.8471 C/\mu\text{M}$
48
49 $+0.1397$, $R^2 = 0.9844$). Where, F_0 represents the fluorescence intensity of blank NBD-TPEA
50
51 solution, and F represents the fluorescent intensity of the mixtures of NBD-TPEA probe and
52
53
54
55
56
57
58
59
60

1
2
3 Zn standards (or the microdialysates for in vivo analysis). The detection limit was calculated
4
5 to be 156 nM ($S/N = 3$). Remarkably, the use of the relative fluorescence intensity (i.e.,
6
7 $(F-F_0)/F_0$) as the signal readout for the calibration eliminates background contamination that
8
9 may be inherent in in vivo sensing of Zn^{2+} (possibly all kinds of trace amount of metal ions)
10
11 in rat brain since the contamination may come from labwares, reagents, and environmental
12
13 contributions within the whole operation procedure.^{14a} To achieve the $(F-F_0)/F_0$ value, in
14
15 conventional fluorescent method, both F and F_0 were read out at the maximum fluorescent
16
17 emission wavelength, which need to be accurately defined under a provided maximum
18
19 excitation wavelength. However, in the method demonstrated here, the easily switchable and
20
21 continuous-flow character of the solutions in the cuvette further facilitates the fluorescent
22
23 signal readout since both the F and F_0 values reach their steady-state values in the
24
25 continuous-flow cell and could be easily defined and read out. Moreover, the
26
27 continuous-flow character of the solutions containing the fluorescence probe in the cuvette
28
29 could minimize the fluorescent bleaching as compared with in the quiescent solution.
30
31
32
33
34
35
36

37 **Application for selective sensing of salicylate-induced Zn^{2+} in rat brain**

38
39 To demonstrate the application of the our method for selectively sensing Zn^{2+} in rat
40
41 brain, we collected the brain microdialysates, pre-mixed the microdialysates with
42
43 NBD-TPEA in DMSO/aCSF (v/v, 1:99, pH 7.4) and perfused the resulting mixture into a
44
45 fluorescent cuvette for continuous-flow fluorescent detection (Scheme 1). As shown in Fig.
46
47 S4 A and Fig. 4 A (black curve), the pre-mixing of 30 μ L of the microdialysate from auditory
48
49 cortex of normal group leads to an obvious increase in the fluorescent intensity, suggesting
50
51 the presence of Zn^{2+} in the auditory cortex microdialysate. The fluorescent intensity remains
52
53 almost unchanged as function of the time from 0 min to 150 min for in vivo microdialysis in
54
55 the auditory cortex, as displayed in Fig. 4 A (black curve), suggesting that the basal level of
56
57
58
59
60

1
2
3 auditory cortex Zn^{2+} does not change in the normal group in the time scale employed in this
4
5 study. The basal level of Zn^{2+} in the auditory cortex microdialysate was determined to be
6
7 $0.52 \pm 0.082 \mu M$ ($n = 4$). To ensure the result obtained with the fluorescent method, we
8
9 further determined the basal level of Zn^{2+} with the traditional ICP-MS, in which the signal
10
11 obtained for aCSF (i.e., without addition of microdialysates) was subtracted to minimize the
12
13 background contamination. We found that the result obtained with our method was almost
14
15 consistent with the value determined with traditional ICP-MS method (i.e., $0.64 \pm 0.10 \mu M$,
16
17 $n = 4$). We shall note that, the basal level of Zn^{2+} in the brain microdialysates reported so far
18
19 remain different, ranging from 19 nM to several hundred nanomolar or even higher.¹⁴ The
20
21 difference might be due to the difference in animal models, brain regions, and experimental
22
23 conditions (for example, the probes and perfusion rates used for in vivo microdialysis)
24
25 employed for in vivo sensing of Zn^{2+} , as reported previously.¹⁴
26
27
28
29

30
31 To further study the change of Zn^{2+} level induced by salicylate, 100 mg/mL of sodium
32
33 salicylate in phosphate buffer (0.1 M, pH 7.4) was intraperitoneally injected into the animals
34
35 (350 mg/kg, i.p.). This dose of sodium salicylate has been reported to be able to induce
36
37 tinnitus.^{2a,3a} The microdialysates were analyzed with the method with the same procedures
38
39 employed for those sampled from the normal animals. As illustrated in Fig. S4 B and Fig. 4
40
41 A (blue curve), the injection of salicylate into the animals leads to an increase in the level of
42
43 extracellular Zn^{2+} in auditory cortex microdialysate from the point of 60 min. The level of
44
45 Zn^{2+} reaches its maximum (i.e., $1.20 \pm 0.24 \mu M$, $n = 4$) at the time point of 90 min and then
46
47 levels off with time after salicylate injection. Previous attempts have demonstrated that the
48
49 development of salicylate-induced tinnitus was a slow process,^{4a,b} and the results obtained
50
51 here suggest that Zn^{2+} in auditory cortex might be involved in the development of
52
53 salicylate-induced tinnitus.
54
55
56

57 To further confirm the involvement of auditory cortex Zn^{2+} in the development of
58
59
60

1
2
3
4 salicylate-induced tinnitus, we injected 1 mg/mL of MK-801, a potent and specific NMDA
5
6 receptor antagonist that blocks both the excitatory and toxic actions of NMDA,¹⁵ into the
7
8 animals (5 mg/kg, i.p., in 0.1 M phosphate buffer, pH 7.4) after the injection of 100 mg/mL
9
10 of salicylate in phosphate buffer (0.1 M pH 7.4) for 5 min (Sal/MK-801 group) and the
11
12 concentration of Zn²⁺ in the microdialysate was detected with the SPM-CFFD method with
13
14 the same procedures for the salicylate group. As illustrated in Fig. S4 C and Fig. 4 A (red
15
16 curve), the concentration of Zn²⁺ in the microdialysates of the MK-801 group first increases
17
18 from 0 min to 90 min, and then decreases after 90 min. This change was rather different from
19
20 the results obtained for the salicylate group, suggesting that the salicylate-induced increase
21
22 in the extracellular Zn²⁺ level was suppressed after the injection of MK-801.
23
24

25
26 For better comparison, we summarized the auditory cortex Zn²⁺ levels of normal,
27
28 salicylate, and Sal/MK-801 groups recorded with our SPM-CFFD method. As illustrated in
29
30 Fig. 4 B, the auditory cortex Zn²⁺ level does not significantly increase both in salicylate
31
32 (blue bars) and Sal/MK-801 (black bars) group at the time point of 30 min, as compared with
33
34 basal levels of normal group (white bars). However, the auditory cortex Zn²⁺ levels in both
35
36 salicylate and Sal/MK-801 groups increase obviously from 60 min to 150 min, as compared
37
38 with basal levels of normal group. Two-way ANOVA followed by a post hoc Tukey test
39
40 indicated significant differences at each time points (from 60 min to 150 min) between
41
42 salicylate group and normal group, and between Sal/MK-801 group and normal group (F
43
44 =30.46, $P < 0.01$; $P = 0.01$, $F_{(5, 18)} = 2.77$). Note that, at the time point of 90 min, although
45
46 the auditory cortex Zn²⁺ level of Sal/MK-801 group was higher than that of salicylate group,
47
48 there is no significant difference between salicylate group and Sal/MK-801 group. At the
49
50 time point of 120 min, there were significant differences in the auditory cortex Zn²⁺ levels
51
52 among normal group, salicylate group and Sal/MK-801 group. These results demonstrated
53
54 that the attenuation of the salicylate-induced increase of auditory cortex Zn²⁺ level is mainly
55
56
57
58
59
60

1
2
3 caused by the intraperitoneal injection of MK-801. It has been reported that, MK-801, as an
4 NMDA receptor antagonist, is competitive to combine with NMDA rather than common
5 neurotransmitters such as glutamate.¹⁵ We speculated that the injection of MK-801 may
6 effectively reduce the NMDA receptor excitotoxicity and eventually inhibit the oxidative
7 damage of auditory cortex and, as a result, attenuate the salicylate-induced increase of the
8 extracellular Zn^{2+} level in the auditory cortex. These results demonstrate that the SPM-CFFD
9 method developed here could be used for in vivo sensing of Zn^{2+} in the cerebral system and
10 will find interesting applications in the investigations on brain functions.
11
12
13
14
15
16
17
18
19
20
21
22

23 **Conclusion**

24
25 By using NBD-TPEA as the selective fluorescence probe and in vivo microdialysis as
26 the sampling technique, we have successfully developed a fluorescent method for in vivo
27 sensing of extracellular Zn^{2+} level in auditory cortex and its change induced by salicylate. To
28 accomplish in vivo fluorescence sensing with simple signal readout recording, minimal
29 fluorescent bleaching, less background contamination and acceptable time resolution, the
30 microdialysates continuously sampled from auditory cortex were pre-mixed with the
31 NBD-TPEA probe, and the mixtures were perfused into a fluorescent cuvette for
32 continuous-flow fluorescence detection to form a new method. The method is highly
33 selective and sensitive for sensing of dynamic change in the Zn^{2+} level in the brain
34 microdialysates and will find interesting applications in the investigations on brain functions.
35
36
37
38
39
40
41
42
43
44
45
46
47

48 **Acknowledgements**

49
50 We acknowledge financial support from the National Natural Science Foundation of
51 China (21321003, 21210007, 21127901, 91213305, and 91232000 for L.M., and 21175141
52 for L.Y.), the National Basic Research Program of China (the 973 programs 2010CB33502
53 and 2013CB933704), and Chinese Academy of Sciences.
54
55
56
57
58
59
60

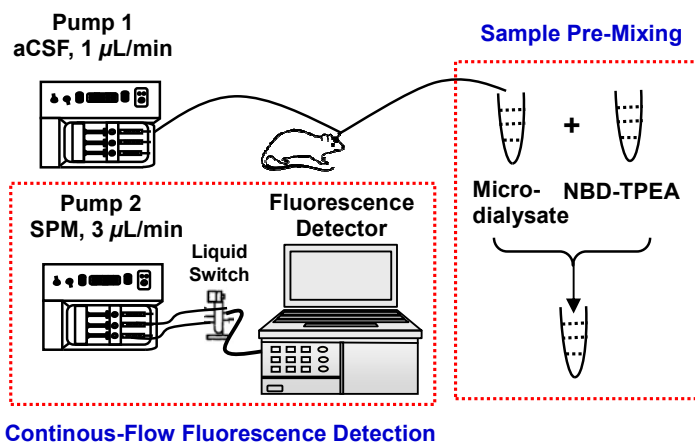
References

- 1 W. Sun, J. Lu, D. Stolzberg, L. Gray, A. Deng, E. Lobarinas and R. Salvi, *J. Neurosci.*, 2009, **159**, 325-334; (b) N. Gong, M. Zhang, X. Zhang, L. Chen, G. Sun and T. Xu, *Neuropharm.*, 2008, **54**, 454-463.
- 2 (a) J. Ruel, C. Chabbert, R. Nouvian, R. Bendris, M. Eybalin, C. L. Leger, J. Bourien, M. Mersel and J. L. Puel, *J. Neurosci.*, 2008, **29**, 7313-7323; (b) M. J. Guitton, J. Caston, J. Ruel, R. M. Johnson, R. Pujol and J. L. Puel, *J. Neurosci.*, 2003, **9**, 3944-3952.
- 3 (a) G. Yang, E. Lobarinas, L. Zhang, J. Turner, D. Stolzberg, R. Salvi and W. Sun, *Hear. Res.*, 2007, **226**, 244-253; (b) M. Zhi, J. T. Ratnanather, E. Ceyhan, A. S. Popel and W. E. Brownell, *Hear. Res.*, 2007, **228**, 95-104.
- 4 (a) M. Knipper, M. Müller and U. Zimmermann, *Springer Handbook of Audi. Res. Chapter 3*; Springer: New York, 2012, 47; (b) J. J. Eggermont and M. Kenmochi, *Hear. Res.*, 1998, **117**, 149-160; (c) D. Oliver, D. Z. He, N. Klocker, J. Ludwig, U. Schulte, S. Waldegger, J. P. Ruppertsberg, P. Dallos and B. Fakler, *Science*, 2001, **292**, 2340-2343.
- 5 (a) J. Ruel, J. Wang, G. Rebillard, M. Eybalin, R. Lloyd, R. Pujol and J. L. Puel, *Hear. Res.*, 2007, **227**, 19-27; (b) K. Tabuchi, B. Nishimura, S. Tanaka, K. Hayashi, Y. Hirose and A. Hara, *Curr. Neuropharmacol.*, 2010, **8**, 128-134.
- 6 J. Liu, P. Yu, Y. Lin, N. Zhou, T. Li, F. Ma and L. Mao, *Anal. Chem.*, 2012, **84**, 5433-5438.
- 7 (a) R. J. Radford and S. J. Lippard, *Curr. Opin. Chem. Biol.*, 2013, **17**, 129-136; (b) S. L. Sensi, P. Paoletti, A. I. Bush and I. Sekler, *Nature Rev. Neurosci.*, 2009, **10**, 780-789; (c) C. J. Frederickson, J. Y. Koh and A. I. Bush, *Nature Rev. Neurosci.*, 2005, **6**, 449-462; (d) L. C. Costello and R. B. Franklin, *J. Biol. Inorg. Chem.*, 2011, **16**, 3-8; (e) S. C. Burdette and S. J. Lippard, *Proc. Natl. Acad. Sci. U.S.A.*, 2003, **100**, 3605-3610; (f) C. B. Coelho, R. Tyler and M. Hansen, *Prog. Brain Res. Chapter 26*, 2007, **166**, 279-285.

- 1
2
3
4 8 (a) A. Takeda, S. Takefuta, S. Okada and N. Oku, *Brain Res.*, 2000, **859**, 352-357; (b) S.
5
6 W. Suh, S. J. Won, A. M. Hamby, B. H. Yoo, Y. Fan, C. T. Sheline, H. Tamano, A.
7
8 Takeda and J. Liu, *J. Cere. Blood Flow & Meta.*, 2009, **29**, 1579-1588; (c) K. M. Dean,
9
10 Y. Qin and A. E. Palmer, *Biochim. Biophys. Acta.*, 2012, **1823**, 1406-1415; (d) P. Paoletti,
11
12 A. M. Vergnano, B. Barbour and M. Casado, *Neuroscience*, 2009, **158**, 126-136; (e) J.
13
14 Qian and J. L. Noebels, *J. Physiol.*, 2005, **566**, 747-758; (f) J. Qian and J. L. Noebels, *J.*
15
16 *Neurosci.*, 2006, **26**, 6089-6095.
- 17
18
19 9 (a) G. Wei, C. J. Hough, Y. Li and J. M. Sarvey, *Neuroscience*, 2004, **125**, 867-877; (b)
20
21 R. B. Thompson, W. O. Whetsell Jr., B. P. Maliwal, C. A. Fierke and C. J. Frederickson,
22
23 *J. Neurosci. Methods*, 2000, **96**, 35-45; (c) S. Ueno, M. Tsukamoto, T. Hirano, K.
24
25 Kikuchi, M. K. Yamada, N. Nishiyama, T. Nagano, N. Matsuki and Y. Ikegaya, *J. Cell*
26
27 *Biol.*, 2002, **158**, 215-220.
- 28
29
30 10 (a) F. J. Jimenez-Jimenez, J. A. Molina, M. V. Aguilar, I. Meseguer, C. J. Mateos-Vega,
31
32 M. J. Gonzalez-Munoz, F. Bustos, A. Martinez-Salio, M. Orti-Pareja, M. Zurdo and M.
33
34 C. Martinez-Para, *J. Neural Transm.*, 1998, **105**, 497-505; (b) A. P. Jayasooriya, M. L.
35
36 Ackland, M. L. Mathai, A. J. Sinclair, H. S. Weisinger, R. S. Weisinger, J. E. Halver, K.
37
38 Kitajka and L. G. Puskas, *Proc. Natl. Acad. Sci. U.S.A.*, 2005, **102**, 7133-7138. (c) T.
39
40 Hirano, K. Kikuchi, Y. Urano, and T. Nagano, *J. Am. Chem. Soc.*, 2002, **124**, 6555-6562.
41
42 (d) K. R. Gee, Z. L. Zhou, W. J. Qian, and R. Kennedy, *J. Am. Chem. Soc.*, 2002, **124**,
43
44 776-778. (e) P. K. Lee, W. H-T. Law, H. W. Liu, and K. K-W. Lo, *Inorg. Chem.* 2011, **50**,
45
46 8570-8579. (f) R. H. Yang,; K. A. Li, K. M. Wang, F. L. Zhao, and F. Liu, *Anal. Chem.*
47
48 2003, **75**, 612-621.
- 49
50
51
52 11 F. Qian, C. Zhang, Y. Zhang, W. He, X. Gao, P. Hu and Z. Guo, *J. Am. Chem. Soc.*, 2009,
53
54 **131**, 1460-1468.
- 55
56
57 12 (a) K. Liu, Y. Lin, L. Xiang, P. Yu, L. Su and L. Mao, *Neurochem. Int.*, 2008, **52**,
58
59
60

- 1
2
3
4 1247-1255; (b) K. Liu, Y. Lin, P. Yu and L. Mao, *Brain Res.*, 2009, **1253**, 161-168; (c) K.
5
6 Liu, P. Yu, Y. Lin, Y. Wang, T. Ohsaka and L. Mao, *Anal. Chem.*, 2013, **85**, 9947-9954;
7
8 (d) M. Zhang, P. Yu and L. Mao, *Acc. Chem. Res.*, 2012, **45**, 533-543.
9
10 13 G. Paxinos and C. Watson, *The Rat Brain in Stereotaxic Coordinates*, 3rd ed.; Academic
11
12 Press: New York, 1997.
13
14 14 (a) C. J. Frederickson, L. J. Giblin, A. Krezel, D. J. McAdoo, R. N. Muelle, Y. Zeng, R.
15
16 V. Balaji, R. Masalha, R. B. Thompson, C. A. Fierke, J. M. Sarvey, M. Valdenebro, D. S.
17
18 Prough and M. H. Zornow, *Exp. Neurol.*, 2006, **198**, 285-293; (b) D. Yang, J. Lee, M.
19
20 Lin, Y. Huang, H. Liu, Y. Liang and F. Cheng, *J. Am. Coll. Nutr.*, 2004, **23**, 552S-555S;
21
22 (c) Y. Kitamura, Y. Iida, J. Abe, M. Mifune, F. Kasuya, M. Ohta, K. Igarashi, Y. Saito
23
24 and H. Saji, *Brain Res. Bull.*, 2006, **69**, 622-625; (d) Y. Kitamura, Y. Iida, J. Abe, M.
25
26 Mifune, F. Kasuya, M. Ohta, K. Igarashi, Y. Saito and H. Saji, *Biol. Pharm. Bull.*, 2006,
27
28 **29**, 821-823; (e) C. J. Frederickson, *Int. Rev. Neurobiol.*, 1989, **31**, 145-238.
29
30
31
32 15 D.W. Choi and S. M. Rothman, *Annu. Rev. Neurosci.*, 1990, **13**, 171-182.
33
34
35
36
37
38
39
40
41
42
43
44
45
46
47
48
49
50
51
52
53
54
55
56
57
58
59
60

Scheme 1



Scheme 1. Schematic illustration of sample pre-mixing and continuous-flow fluorescent detection for in vivo sensing of Zn^{2+} .

Fig. 1

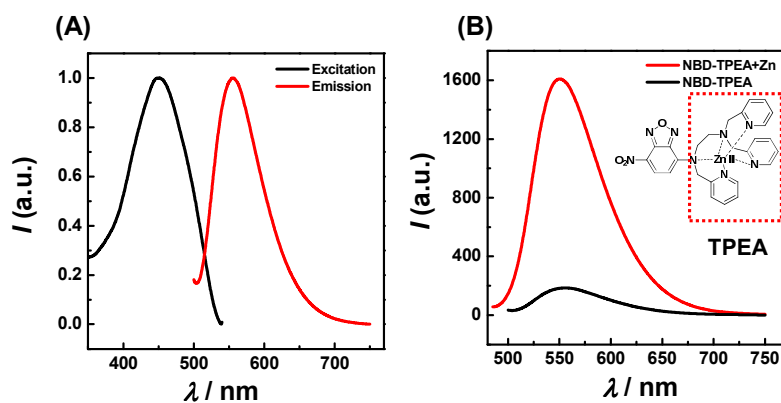


Fig. 1 (A) Excitation (black curve) and emission (red curve) spectra of 10 μM of NBD-TPEA in DMSO/aCSF (v/v, 1:99, pH 7.4). (B) Fluorescent emission spectra of 10 μM of NBD-TPEA in the absence (black curve) and presence (red curve) of 10 μM of Zn²⁺ in DMSO/aCSF (v/v, 1:99, pH 7.4). Inset, the proposed binding mode of Zn²⁺ with NBD-TPEA.

Fig. 2

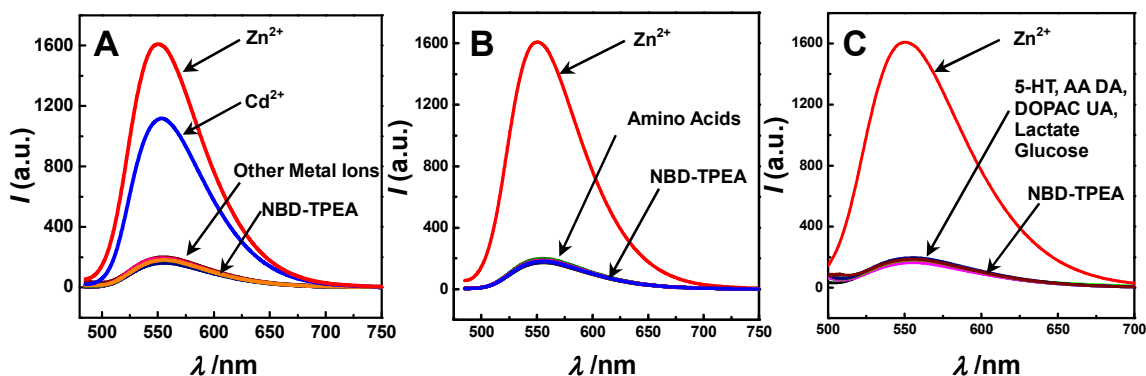


Fig. 2 (A) Fluorescence emission spectra of 10 μM of NBD-TPEA in the absence (black curves) and presence of each kind of metal ions (A), amino acids (B), and physiologically important species (C) in DMSO/aCSF (v/v, 1:99, pH 7.4). $\lambda_{\text{ex}} = 469$ nm. The concentrations for metal ions were 100 μM for K^+ , Na^+ , Ca^{2+} , Mg^{2+} , and 10 μM for other metal ions. The concentrations of each kind of amino acids were 100 μM . The concentrations for physiologically important species were 5-HT (10 μM), AA (200 μM), DA (10 μM), DOPAC (10 μM), glucose (10 mM), lactate (1 mM) or UA (80 μM). Black curve overlaps with the curves with the colors rather than blue and red. $\lambda_{\text{ex}} = 469$ nm.

Fig. 3

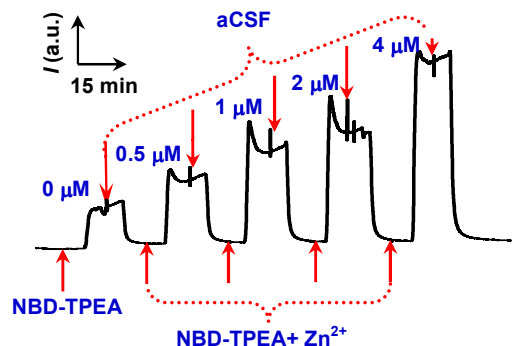


Fig. 3 Typical fluorescence-time response obtained with the method for the Zn²⁺ standards. A 30 μL of different concentrations of Zn²⁺ in aCSF (pH 7.4) was pre-mixed into 30 μL of NBD-TPEA (10 μM) in DMSO/aCSF (v/v, 1:99, pH 7.4) for 5 min, and the resulting mixtures were perfused into a fluorescent cell for continuous-flow fluorescent detection. Flow rate, 3 μL min⁻¹. The final concentrations of Zn²⁺ were indicated in the figure.

Fig. 4

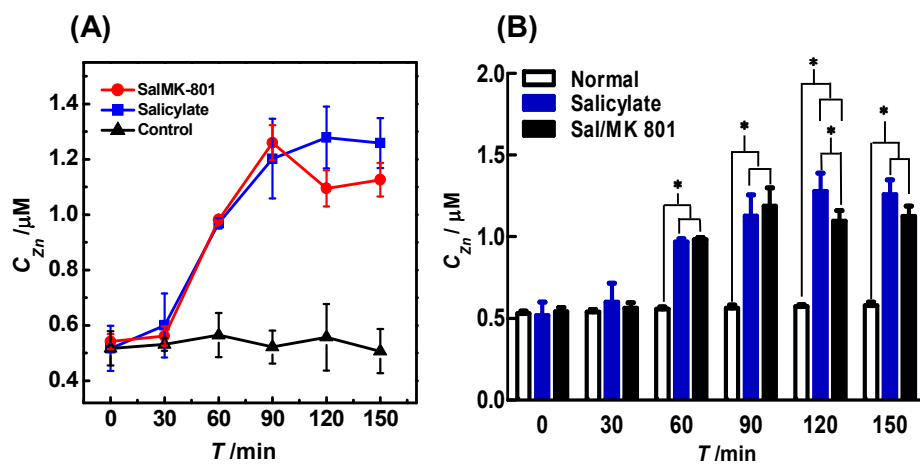


Fig. 4 (A) Dynamic changes of auditory cortex Zn²⁺ in the normal (black curve), salicylate (blue curve) and Sal/MK-801 (red curve) groups ($n = 4$). All brain microdialysates (with a perfusion rate of $1 \mu\text{L min}^{-1}$) were pre-mixed with $30 \mu\text{L}$ of NBD-TPEA ($10 \mu\text{M}$) in DMSO/aCSF (v/v, 1:99, pH 7.4) for 5 min, and the resulting mixtures were perfused into a fluorescent cell for continuous-flow fluorescent detection. Perfusion rate for the mixtures was $3 \mu\text{L min}^{-1}$. Other conditions were the same as those in Fig. 3. (B) Comparison of the dynamic changes of auditory cortex Zn²⁺ levels of normal group (white bars), salicylate group (blue bars), and Sal/MK-801 group (black bars). Data presented as mean \pm SD. The asterisks ($*P < 0.01$.) indicate significant differences among auditory cortex Zn²⁺ levels of normal group, salicylate group, and Sal/MK-801 group.

Table of Content

